

A. STEFANIK<sup>\*,#</sup>, A. MOREL<sup>\*</sup>, S. MRÓZ<sup>\*</sup>, P. SZOTA<sup>\*</sup>

## THEORETICAL AND EXPERIMENTAL ANALYSIS OF ALUMINIUM BARS ROLLING PROCESS IN THREE-HIGH SKEW ROLLING MILL

### TEORETYCZNO – DOŚWIADCZALNA ANALIZA PROCESU WALCOWANIA PRĘTÓW ALUMINIOWYCH W TRÓJWALCOWEJ WALCARCE SKOŚNEJ

Technology of round bars rolling on a three-high skew rolling mills allows rolling of standard materials such as steel and aluminum, as well as new materials, especially hard deformable materials. The paper presents the results of theoretical and experimental rolling process of aluminum bars with a diameter of 20 mm. As the stock round bars with a diameter of 25 mm made of aluminum grade 1050A and aluminum alloy grade 2017A were used. The rolling process of aluminum bars has been carried out in a single pass. The numerical analysis was carried out by using computer program Forge2011®. On the basis of theoretical research it has been determined the state of deformation, stress and temperature distribution during rolling of aluminum bars. In addition, the results of theoretical research allowed to determine the schema of the metal plastic flow in the roll gap. Verification of the theoretical research was carried out during the rolling of aluminum bars on the RSP 40/14 laboratory three-high skew rolling mill. From the finished bars were taken the samples to set the shape and compared with the results of theoretical research. Finished aluminum round bars were characterized by low ovality and good surface quality.

*Keywords:* three-high skew rolling mill, aluminum alloys, round bars, FEM, numerical analysis

Technologia walcowania prętów okrągłych w trójwalcowych walcarkach skośnych pozwala na wytwarzanie prętów zarówno ze standardowych materiałów, takich jak stal i aluminium, jak również prętów z nowych materiałów, zwłaszcza materiałów trudno odkształcalnych. W artykule przedstawiono wyniki badań teoretycznych oraz doświadczalnych procesu walcowania prętów aluminiowych o średnicy 20 mm. Jako wsad zostały zastosowane pręty okrągłe o średnicy 25 mm z aluminium w gatunku 1050A oraz stopu aluminium w gatunku 2017A. Proces walcowania prętów aluminiowych przeprowadzono w jednym przebiegu. Badania teoretyczne wykonano stosując program komputerowy Forge2011®. Na podstawie wyników badań teoretycznych określono stan odkształcenia, naprężenia oraz rozkład temperatury podczas walcowania prętów aluminiowych. Ponadto uzyskane wyniki badań teoretycznych umożliwiły określenie schematu plastycznego płynięcia metalu w kotlinie walcowniczej. Weryfikację badań teoretycznych przeprowadzono podczas walcowania prętów aluminiowych na trójwalcowej walcierce skośnej RSP 40/14. Z gotowych prętów aluminiowych o średnicy 20 mm pobrano templety, których kształt porównano z wynikami badań teoretycznych. Gotowe pręty charakteryzowały się małą owalnością oraz dobrą jakością powierzchni.

### 1. Introduction

In recent years, the application of aluminum alloys to structural components in aerospace and ground vehicles is increasing due to its excellent properties such as low density, high specific strength and stiffness, good machinability and castability [1, 2]. At the same time increasing competition in global markets, forces among manufacturers seek new methods of providing cost reductions while maintaining or even improving the quality of finished products.

Currently, aluminum bars are produced mainly by extrusion [3]. One of the modern methods of production of bars is rolling in three-high skew rolling mill [4-7]. This method allows the rolling of standard materials such as steel and aluminum, as well as for hard deformation materials such as magnesium alloys. Three-high skew rolling process allows a large

reduction in the diameter of the bars rolled in one pass, while keeping high quality of the surface and roundness of the finished product. Besides rolling in three-high skew rolling mill process can ensure the production of bars of comparable properties at lower cost [8]. The process of rolling on a three-high rolling mill is complicated due to the complex strain and stress state prevailing in the roll gap. This state is influenced by a number of parameters, including: rolling speed, roll diameter, band temperature, roll axis inclination angle [4, 7].

The main purpose of this paper were theoretical analysis of aluminum 1050A and aluminium alloy 2017A bars rolling in three-high skew rolling mill process and experimental verification of the used theoretical model. On the basis of theoretical research it has been determined the state of deformation, stress and temperature distribution during rolling of aluminum bars. In addition, the results of theoretical research allowed to

\* CZESTOCHOWA UNIVERSITY OF TECHNOLOGY, FACULTY OF PRODUCTION ENGINEERING AND MATERIALS TECHNOLOGY, THE INSTITUTE OF METAL FORMING AND SAFETY ENGINEERING, 19 ARMII KRAJOWEJ STR., 42-200 CZĘSTOCHOWA, POLAND

# Corresponding author: stefanik@wip.pcz.pl

determine the schema of the metal plastic flow in the roll gap. In the Figure 1 are shown three-high skew rolling mill RSP 14/40 which is located in The Institute of Metal Forming and Safety Engineering Czestochowa University of Technology (CUT) used for aluminum bars rolling process and FE model used for numerical analysis. A characteristic feature of RSP 14/40 three-high skew rolling mill is that the roll axis inclination angle is  $18^\circ$ , while the conventional three-high skew rolling mills which are used to the tubes and bars production, in the maximum axis inclined angle is  $16^\circ$  [9], this ensures better stability of the rolling process.

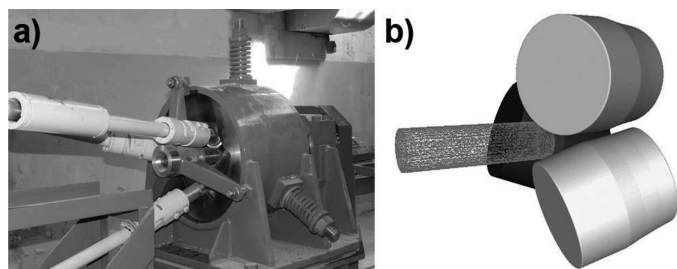


Fig. 1. View of three-high skew rolling mill – a), and FE model used for the numerical modelling – b)

## 2. The properties of materials used in the research

The stock materials were aluminium grade 1050A and aluminium alloy grade 2017A (according to the EU standard) widely used in various industry branches, which chemical composition is given in Table 1.

TABLE 1  
Chemical composition of 1050A and 2017A aluminium alloys /%

	Al	Cu	Pb	Fe	Si	Mn	Mg
<b>1050A</b>	99.7	0.002	-	0.18	0.06	0.03	0.02
<b>2017A</b>	92.1	3.8	0.9	0.3	0.5	0.7	0.6

The application of the computer program Forge2011® using the thermo-mechanical models that it contains requires the definition of boundary conditions which are decisive to the correctness of numerical computation. The accuracy of numerical modelling highly depends on the accurate determination of the properties of materials used for simulations. The yield stress  $\sigma_p$  dependence of strain  $\varepsilon$ , strain rate  $\dot{\varepsilon}$  and temperature  $T$  used for the theoretical research is approximated by extended Hensel-Spittel [10] formula expressed as:

$$\sigma_p = A \cdot e^{m_1 \cdot T} \cdot T^{m_9} \cdot \varepsilon^{m_2} \cdot e^{\frac{m_4}{\varepsilon}} \cdot (1 + \varepsilon)^{m_5 \cdot T} \cdot e^{m_7 \cdot \varepsilon} \cdot \dot{\varepsilon}^{m_3} \cdot \varepsilon^{m_8 \cdot T}, \text{ MPa} \quad (1)$$

where:  $A$ ,  $m_1 \div m_9$  – coefficient of the function

In order to determine the coefficients of the equation (1) performed approximation results of the plastometric test results made on the Gleeble 3800 system in Institute of Metal Forming and Safety Engineering CUT. Plastometric tests were performed, using strain rate of:  $0.1 \text{ s}^{-1}$ ,  $1.0 \text{ s}^{-1}$ , and  $10.0 \text{ s}^{-1}$  for the temperature range  $300 \div 500^\circ\text{C}$  for both materials.

Coefficients used in equation (1) for both materials are given in Table 2. Example flow curves for the aluminum grade 1050A and aluminum alloy grade 2017A for the temperature  $400^\circ\text{C}$  (initial temperature of the stock in rolling process) are presented in Fig. 2. As it can be noticed for the corresponding value to the strain rate yield stress value for the aluminum alloy grade 2017A is more than two fold higher than for aluminum grade 1050A. The other properties of the aluminum alloys used in research were determined on the basis of the literature [11, 12].

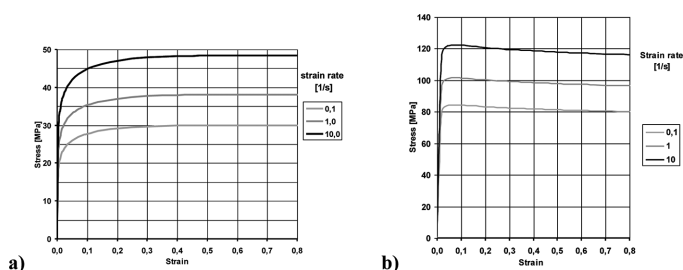


Fig. 2. Plastic flow curves at a temperature of  $400^\circ\text{C}$  for a) aluminum grade 1050A, b) aluminum alloy grade 2017A

## 3. Numerical modelling of the aluminum bars rolling process in three-high skew rolling mill

A computer program Forge2011® has been repeatedly used in the modelling of forming processes. With appropriate selection of the initial parameters, obtained results were characterized by a high compatibility with experimental research [13-15]. For performing the numerical computation of the bars rolling process in the three-high skew rolling mill a three-dimensional model was designed in a CAD-type program. This model was surface objects, whose surfaces were then transformed into a finite-element mesh. The computer program Forge2011® utilizes models built from a finite-element mesh, whose base element is a triangle. For the tool model, a three-dimensional surface mesh was used. While for the object being deformed a spatial mesh was generated based on the surface mesh. The finished spatial mesh in the object being deformed is built from tetrahedral elements and its size is characterized by defining the mean edge length.

Parameters of function (1) for: the 1050A and 2017A

TABLE 2

	$A_0$	$m_1$	$m_2$	$m_3$	$m_4$	$m_5$	$m_7$	$m_8$	$m_9$
<b>1050A</b>	0.08743	-0.009930	0.113250	-0.08845	-0.00058	-0.00153000	0.19627	0.00048	1.71527
<b>2017A</b>	680.5	-0.004846	-0.022011	0.080719	-0.000535	-0.0000002215	-0.014184	0.00000012	-0.001342

The working rolls were designed based on technical documentation of three-high skew rolling mill. Due to the complexity of the mill in order to properly determine the position of the working rolls was necessary to build a model including a movable body and inserts with fixed working rolls. Based on designed three-high skew rolling mill CAD model it was possible to determine the position and the axis of the working rolls rotation. The prepared working tools and stock model were then arranged according to the adopted rolling conditions in three-high skew rolling mill (Figure 1b). In order to determine the bars twisting during deformation in the roll gap, sensors were introduced respectively representing the distances  $r$  (A),  $2/3r$  (B), and  $1/3r$  (C), (where  $r$  – the radius of the stock) to allow archiving of the coordinates during rolling process.

An initial diameter of the stock was 25 mm. The diameter of the final bars was set up to 20 mm. Elongation in this case during the aluminum bar rolling in three-high skew rolling mill was 1.56. The theoretical analysis was performed for the real rolling conditions: the working rolls speed of 100 rpm, friction factor – 0.8, coefficient of heat exchange between the material and the tool  $\alpha - 3\ 000\ \text{W/Km}^2$ ; coefficient of heat exchange between the material and the air  $\alpha_{air} - 10\ \text{W/Km}^2$ , working rolls temperature –  $50^\circ\text{C}$ ; ambient temperature –  $20^\circ\text{C}$  and the stock temperature –  $400^\circ\text{C}$ , working rolls diameter – 150 mm.

#### 4. Results of the numerical modelling and discussion

The distribution of stress, effective strain and temperature within the roll gap are shown in five band cross-sections (Figures 4-6). The first cross-section (I) corresponds to the entry material to roll gap, the last cross-sections (V) is located on the plane of exit from the roll gap (Figure 3). Other cross-sections are located in equal distances. In the Figure 3 is shown example distribution of effective strain during 2017A bars rolling process.

As it can be noticed the maximum values of the effective strain form the characteristic sprains lines on the bar surface. Similar sprain lines can be seen on the finished aluminum bars rolled in laboratory conditions.

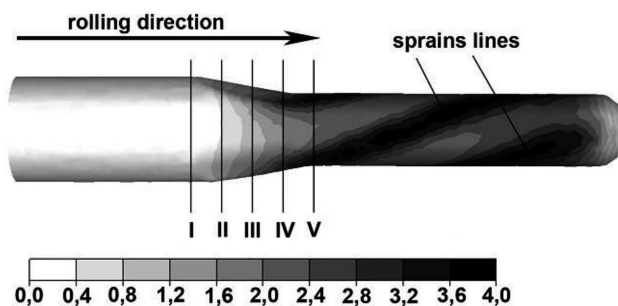


Fig. 3. Distribution of effective strain – view of the characteristic lines sprains during the 2017A bar rolling in three-high skew rolling mill

In the Figure 4 is shown the distribution of effective stress during the 25 mm round bars in three-high skew rolling mill. From the data shown in Figure 4 it can be found that the highest effective stress values occur at the locations of band contact with the rolls and are equal to approx. 70 MPa (1050A), and

approx. 160 MPa (2017A). In the first stage of rolling in the zone of metal entry to the roll gap, the stress increase and, as the band moves along the roll gap, the value of effective stress increases to reach maximum values in the central part of the band. As the band moves along the roll gap, the strain builds up. This causes an increase in the values of effective strain. This is due to the conditions of deformation in the three-high skew rolling mill. The inclination of the roll axes in two planes during rolling causes band bending and contributes to obtaining large deformations in a single pass.

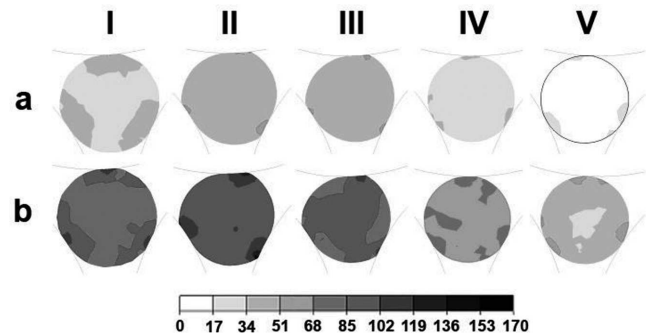


Fig. 4. Distribution of effective stress during the 25 mm round bar rolling in three-high skew rolling mill: a) 1050A, b) 2017A

The data in Figure 5 indicate that at the moment of roll bite the band only contacts pointiest with each of the working rolls. Along with the band moving across the roll gap, the strain grows, which causes an increase in the values of effective strain (Figure 5). The highest effective strain values occur within the outer material areas. The value of effective strain in the central area is lower compared to the outer area of the band.

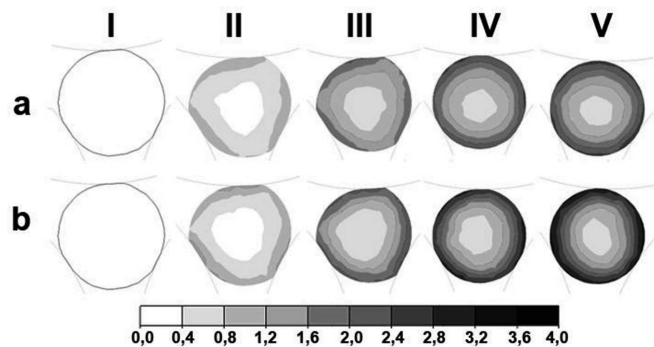


Fig. 5. Distribution of effective strain during the 25 mm round bar rolling in three-high skew rolling mill: a) 1050A, b) 2017A

It can be noticed that the highest value of effective strain is approx. 3.8 for the 2017A bars and 2.5 for the 1050A bars in the outer zone, in the central zone the value is approx. 0.6 for both materials, which means for this ratio of the bar diameter reduction during the rolling deformation occurs throughout the cross-section of the rolled aluminum bar. Deformation in the central area is caused by the shear stress brought about forced sprain rolled bar during three-high skew rolling process.

The temperature distribution during the skew rolling process of aluminum bars in specified cross-section is presented in Figure 6.

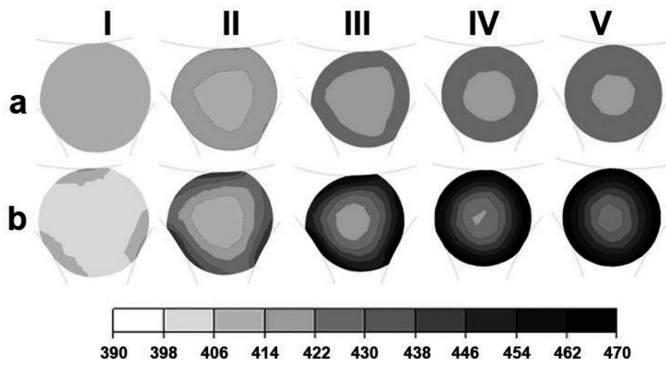


Fig. 6. Distribution of temperature during the 25 mm round bar rolling in three-high skew rolling mill: a) 1050A, b) 2017A

Analyzing the data presented in Figure 6 it can be seen an increase the temperature that occurs during the rolling in both used materials. The greatest rise in temperature is observed in the outer areas of rolled bars, where the values of effective strain are greatest. As it can be seen during the 2017A bars rolling the temperature increases up to approx. 70°C and for the 1050A it's approx. 30°C. Temperature increase is closely related to a given deformation during the rolling process, in which deformation energy is transformed into thermal energy causing an increase temperature of deformable material. Due to the kinematics of the skew rolling process band that moves linearly and rotates on its own axis a local contact of deformed metal with working rolls is short enough that it does not permit the transfer of the heat generated to the rolls.

Based on established values recorded in the stock sensors twisting angle of the rolled bars in the roll gap has been determined. The sprains lines of the rolled bar in the roll gap and values of twisting angle determined for the assumed sensors for both rolled aluminum bars are presented in Figure 7.

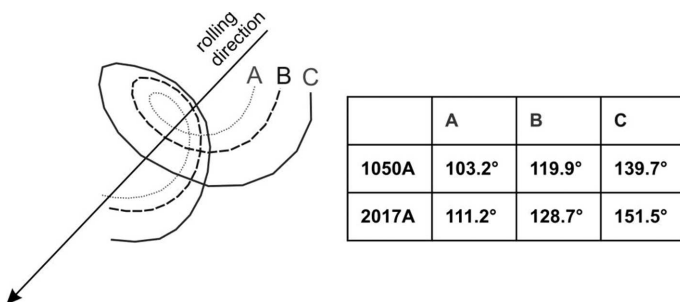


Fig. 7. Sprains lines oblique designated for the characteristic points A, B and C aluminium bars rolled in a three-high skew rolling mill

Analyzing the data presented in Fig. 7 it can be seen that the twist angle is different depending on the distance deformable point of the longitudinal axis of rotation of the band. It can be also noticed that the twisting angles determined during the numerical modelling of the 2017A aluminum alloy rolling process are greater than the twisting angles estimated for 1050A aluminum.

A more detailed analysis allows to determine the difference of the twisting angles of rolled bars in roll gap has been carried out on the basis of the distribution of velocity component of metal plastic flow in the rolling direction ( $v_z$ ). The velocity distribution of the metal plastic flow  $v_z$  the

cross-section located in the upper roll axis has been shown in Fig. 8.

Analyzing the data presented in Figure 8 can notice the difference in the values of the metal flow velocity component in the direction of rolling  $v_z$ . This difference is mainly due to the rheological properties of rolled materials. Aluminum alloy 2017A has more than two higher yield stress as compared to 1050A at the assumed temperature of the rolling process. Based on the data shown in Fig. 8 it can be noticed that in the contact zone rolled aluminum bars with working rolls velocity component  $v_z$  has a much higher value (in the range of 120 to 140 mm/s for the 1050A and 90 to 110 mm/s for the 2017A) than in the areas of the core (80 to 100 mm/s for the 1050A and 60 to 80 mm/s for the 2017A).

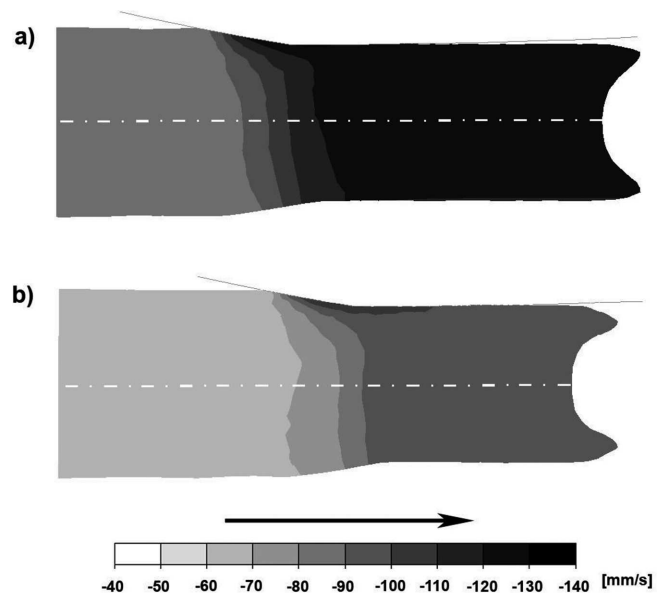


Fig. 8. The distribution of metal plastic flow velocity  $v_z$  on the longitudinal section: a) 1050A, b) 2017A

Result of rotation of the deformed aluminum bar values of the velocity component  $v_z$  are decreased. Hence it can be concluded that with increasing distance the deformable layer of metal from the longitudinal axis of rotation, resulting the displacement of the metal in the rolling direction is higher. This is due to the fact that differentiation of the twisting angle in the roll gap (Fig. 7) and is caused mainly by the fact that for the separate bands twisted metal in the outer areas of the band (sensor A) is greater movement in the rolling direction than in the layers respectively closer the longitudinal axis of rotation of the band.

### 5. Laboratory research of the aluminium round bars rolling process in three-high skew rolling mill

The rolling process of aluminum bars having a diameter of 20 mm was performed on three-high skew rolling mill RSP 14/40. The testing samples were prepared from extruded bars having a diameter of 25 mm and a length of 300 mm which were degreased and pre-sanding with an abrasive agent in order to increase friction between the metal and the deformed working rolls. Parameters for the rolling aluminum bars in three-high skew rolling mill laboratory process were same as

it was assumed numerical studies. The samples were heated in a chamber furnace for 25 minutes to a temperature 400°C. After the rolling process for both rolled materials were taken samples to determine the dimensions of the finished bars, which were then compared with the results of theoretical results. Analysis of rolled aluminum bars in three-high skew rolling mill showed straightness and no surface defects. In the Figure 9 has been presented samples taken from the aluminum bars rolled in three-high skew rolling mill, it can be noticed characteristic sprain lines on the finished bars (compared to sprain lines estimated in theoretical research Figure 3).



Fig. 9. Samples taken from the aluminum bars rolled in three-high skew rolling mill

Comparison of the dimensions estimated in theoretical and laboratory research is presented in Table 3. As can be seen from the results shown in Table 3 for both used materials the difference between maximum and minimum diameters not exceeded 0.5 mm in laboratory test and 0.2 in numerical modelling. After rolling in three-high skew rolling mill round bars have a very small ovality. It may be also notice a high accuracy of the results obtained for the actual process of rolling and numerical modelling. The maximum difference in diameter set in the laboratory and theoretical research does not exceed 0.5 mm.

TABLE 3

Diameters of the 20 mm round bars obtained in the numerical modelling and laboratory tests

	Numerical modelling / mm			Laboratory test / mm		
	min.	max.	$\Delta$	min.	max.	$\Delta$
<b>1050A</b>	20.5	20.6	0.1	20.1	20.4	0.3
<b>2017A</b>	20.4	20.6	0.2	20.1	20.5	0.4

In order to determine the accuracy of the used theoretical model also the total power of the rolling 2017A alloy bars was used. Based on the theoretical studies results total rolling power was 8.3 kW which is about 11 % lower than the values measured during laboratory rolling – 9.2 kW. On this difference may affect both the measurement errors assistive technologies applicable to the study of theoretical parameters of deformed metal. However obtained error can be considered acceptable for the assumed theoretical model.

## 6. Summary

- From the investigation carried out it can be found that:
- rolling on the three-high skew rolling mill allows the rolling process to be run with high elongation factors in a single pass, which makes skew rolling become more economical and reduces the losses for roll mechanical working;
  - the scheme used rolling deformation of the bar is unequal, however, occurs throughout the cross section of the rolled aluminum bar for both used materials;
  - increasing the temperature of aluminum bars during rolling is closely related to a given deformation, increase of the rolled material temperature can be used to reduce the initial material temperature at the beginning of the rolling process;
  - increasing distance the deformable layer of metal from the longitudinal axis of rotation, resulting the displacement of the metal in the rolling direction is higher;
  - in the bars after rolling in three-high skew rolling mill are straight don't have surface defects and have low ovality;
  - application of the three-high skew rolling process to production of aluminum round bars could be alternative to extrusion process.

## REFERENCES

- [1] A. Heinzl, A. Haszlera, C. Keidela, S. Moldenhauerb, R. Benedictusb, W.S. Millerb, *Materials Science and Engineering A* **280**, 120 (2000).
- [2] I.N. Fridlyander, V.G. Sister, O.E. Grushko, V.V. Berstenev, L.M. Sheveleva, L.A. Ivanova, *Metal Science and Heat Treatment* **44**, 365 (2002).
- [3] M. Noorani-Azad, M. Bakhshi-Jooybari, S.J. Hosseini-pour, A. Gorji, *Journal of Materials Processing Technology* **164**, 1572 (2005).
- [4] K. Nakasuji, K. Maruda, C. Hayashi, *ISIJ International* **36**, 572 (1996).
- [5] K. Nakasuji, K. Maruda, C. Hayashi, *ISIJ International* **37**, 899 (1997).
- [6] S. Galkin, H. Dyja, A. Galkin, A. Rząsowska, *Hutnik-Wiadomości Hutnicze* **12**, 589 (2004).
- [7] A. Morel, S. Mróz, A. Stefanik, P. Szota, H. Dyja, *Rudy i Metale Nieżelazne* **11**, 794 (2013).
- [8] A. Rząsowska-Przała, W. Waszkielewicz, A. Gałkin, *Zagadnienia Techniczno-Ekonomiczne* **50**, 169 (2005).
- [9] Z. Pater, J. Kazanecki, *Archives of Metallurgy and Materials* **58**, 717 (2013).
- [10] A. Hensel, T. Spittel, *Kraft und Arbeitsbedarf Bildsomer Formgebungs Verfahren*, Lipsk 1979.
- [11] S. Berski, H. Dyja, A. Maranda, J. Nowaczewski, G. Banaszek, *Journal of Materials Processing Technology* **177**, 582 (2006).
- [12] Z.A. Vasudevan, R. Doherty, *Aluminum Alloys-Contemporary Research and Applications*, San Diego 1989.
- [13] T. Garstka, R. Dobrakowski, B. Koczurkiewicz, H. Dyja, *Journal of Materials Processing Technology* **157**, 159 (2004).
- [14] A. Kawałek, *Journal of Materials Processing Technology* **157**, 531 (2004).
- [15] K. Laber, H. Dyja, M. Kwapisz, *Archives of Metallurgy and Materials* **56**, 385 (2011).